# A SIMPLE METHOD FOR CALCULATING STRESS INTENSITY FACTORS FOR INTERLAMINA CRACKS IN COMPOSITE LAMINATES

Y. Morioka* and C.T. Sun
School of Aeronautics and Astronautics, Purdue University, West Lafayette, USA
* Corresponding author (morioka.yuta@gmail.com)

**Keywords**: *interfacial crack, stress intensity factors, composite materials, finite element method*

## 1 Introduction

In advanced composite materials, one of the major failure modes is delamination. Delamination in composite laminates can be considered as an interfacial crack between two highly anisotropic materials. Unlike a crack in a homogeneous medium, researchers have found the violent oscillatory nature of near-tip stress and displacement fields. It was found by England [4] that the oscillatory displacement fields lead to mutual penetration of upper and lower crack surfaces, which is physically inadmissible. Comninou [5] proposed modifications to the model in order to account for the contact but it involved complicated analyses. Rice [6] has discussed that although oscillatory solutions do not describe near-tip fields accurately, the solutions are valid outside of small scale contact zone. Sun and Qian [7] performed comparison of those two models, and confirmed Rice's argument. Therefore, the oscillatory model can be used to characterize fracture when the contact zone is small compared to fracture process zones. Hence, the oscillatory model was adapted throughout the research.

It was shown by Sun and Qian [1] that strain energy release rates do not exist for interfacial cracks. In addition, Cao and Evans [2] found that fracture toughness of an interfacial crack is a function of mode mixities. Because of these characteristics, stress intensity factors must be computed in order to characterize fracture. Several methods have been proposed by other researchers to compute stress intensity factors for interfacial cracks but they have not been widely used in industries due to complex mathematics involved in the analyses. To make a breakthrough in this situation, a simple method for calculating stress intensity factors is proposed in this paper.

### 2.1 Near-tip Fields

Consider a body consisting of two dissimilar anisotropic media with an interfacial crack as shown in Fig. 2. In this case, near-tip stress and displacement fields were derived by Hwu [3] as

$$\begin{Bmatrix}\sigma_{xy}\\ \sigma_{yy}\\ \sigma_{yz}\end{Bmatrix} = \frac{1}{\sqrt{2\pi x}}\boldsymbol{\Lambda}\langle\langle\left({}^{x}/_{2a}\right)^{i\epsilon_\alpha}\rangle\rangle\boldsymbol{\Lambda}^{-1}\begin{Bmatrix}K_{II}\\ K_I\\ K_{III}\end{Bmatrix} \quad (1)$$

$$\begin{Bmatrix}\Delta U_x\\ \Delta U_y\\ \Delta U_z\end{Bmatrix} = \sqrt{\frac{2x}{\pi}}\left(\overline{\boldsymbol{\Lambda}}^{\boldsymbol{T}}\right)^{-1} \langle\langle\frac{\left({}^{x}/_{2a}\right)^{i\epsilon_\alpha}}{(1+2i\epsilon_\alpha)\cosh(\pi\epsilon_\alpha)}\rangle\rangle\boldsymbol{\Lambda}^{-1}\begin{Bmatrix}K_{II}\\ K_I\\ K_{III}\end{Bmatrix} \quad (2)$$

respectively. In above equations, $\Delta U_i$ ( $i = x, y, z$) indicate the relative crack surface displacements. The angular brackets indicate a 3×3 diagonal matrix, $\epsilon_\alpha$ ($\alpha$=1,2,3) are the bimaterial constants which involve the elastic constants of the two materials, and $\Lambda$ is the eigenvector matrix that appears in the Stroh formalism.

It was shown in [1] that individual strain energy release rates ($G_I$, $G_{II}$, and $G_{III}$) derived based on equations (1) and (2) are also oscillatory and does not converge. Hence, individual strain energy release rates do not exist for interfacial cracks. For cracks in homogeneous media, it is a common practice to determine stress intensity factors by first calculating strain energy release rates then converting them through the *G-K* relationships. Because of the nonexistence of *Gj (j=I,II,III)*, the technique is no longer valid for problems involving interfacial cracks. Since fracture is characterized through stress intensity factors, an alternative approach must be established to find them. In the following section of the paper, a simple method to determine stress intensity factors is proposed.

### 2.2 Projection Method

The stress intensity factors can be determined from (1) by inverting the relationship as

$$\begin{Bmatrix} K_{II} \\ K_I \\ K_{III} \end{Bmatrix} = \lim_{x\to 0}\sqrt{2\pi x}\boldsymbol{\Lambda}\langle\langle\left(x/2a\right)^{i\epsilon_\alpha}\rangle\rangle^{-1}\boldsymbol{\Lambda}^{-1}\begin{Bmatrix} \sigma_{xy} \\ \sigma_{yy} \\ \sigma_{yz} \end{Bmatrix} \quad (3)$$

where stress components $\sigma_{xy}$, $\sigma_{yy}$, and $\sigma_{yz}$ are obtained from finite element analyses. The limit is necessary in accordance to the definition of stress intensity factors. The procedures for the projection method are as follows. First, compute the stresses along the interface ($y=0$) using the finite element method. Then plot each $K_j$ ($j=I,II,III$) as a function of the distance from the crack tip, $x$, according to the equation (3) as illustrated by $P_j$ in Fig. 1. Each plot would be a straight line except for the first few elements near the crack tip as illustrated in the figure. This is due to the high stress gradients near the crack tip, and the stresses computed by the finite element analysis are not accurate in this region. Hence ignoring this part of the plots, project straight lines toward the crack tip ($x=0$) from the portions where plots are straight, as illustrated by dashed lines in Fig. 1. The intersections of each plot with $x=0$ are the stress intensity factors, $K_j$.

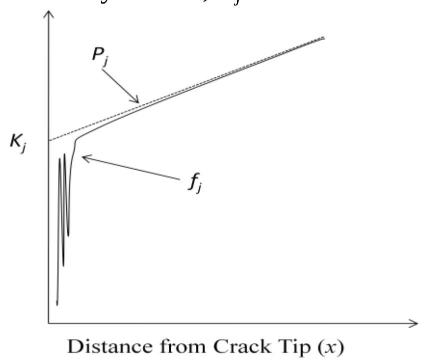


Fig. 1 Illustration of the projection method. Plots need to be drawn for all $K_j$ ($j = I, II, III$)

## 3 Finite Element Analysis

In order to verify the accuracy of the proposed method, a set of finite element analyses was performed. Three example problems are solved using the projection method. The stress intensity factors obtained by the method are compared to those by the displacement ratio method proposed by Sun and Qian [1]. Note that throughout this paper, "//" is used to indicate locations of interfacial cracks.

### 3.1 Infinite Bimaterial Body with a Center Crack along the Interface under Remotely Applied Simple Tension

Consider an infinite body consisting of two dissimilar anisotropic media with a center crack along its interface, as shown in Fig. 2. Those media may be considered as a unidirectional composite lamina stacked in different orientations, $\theta_i (i = 1,2)$. Each ply has two of its principal axes ($x_1$ and $x_2$) on $x$-$z$ plane, and the third principal axis ($x_3$) parallel to $y$. The angle between $x$-axis and $x_1$-axis is denoted by $\theta$. Simple tension, $\sigma_{yy}^{\infty}$, is applied remotely to the body. In this case, stress intensity factors were derived analytically by Hwu [3] as,

$$K_I = \sigma_{yy}^{\infty}\sqrt{\pi a}$$

$$K_{II} = \frac{2a_f\epsilon}{b_f}\sigma_{yy}^{\infty}\sqrt{\pi a}$$

$$K_{III} = -\frac{2d_f\epsilon}{b_f}\sigma_{yy}^{\infty}\sqrt{\pi a}$$

where constants ($a_f, b_f d_f$, and $\epsilon$) are related to material properties of the lamina, and can be found in [1].

Finite element analysis was performed on this problem. The results obtained from the projection method are compared to those from the displacement ratio method and Hwu's analytic solution. Since the analytic solution is based on the infinite body assumption, the finite element model needs to be sufficiently large in order to satisfy the same boundary conditions. In this study, the following geometry was selected: $h=100\ m$, $w=100\ m$, $a=1m$. The material properties of the lamina are $E_1=138GPa$, $E_2=E_3=9.86GPa$, $\nu_{12}= \nu_{13}=\nu_{23}=0.3$, $G_{12}=G_{13}=G_{23}=5.24GPa$. The applied load of $\sigma_{yy}^{\infty}=1Pa$ was used in the numerical analysis. Since the loading is independent of $z$-direction, the problem may be considered to be in generalized plane strain condition. This condition was modeled in finite element analyses by having only one element in $z$-direction, and applied periodic boundary conditions on corresponding nodes on front and back faces of the body. The 20-node brick element was used, and the mesh was refined near the crack tip. Structured mesh needs to be used when using the displacement ratio method because it requires computation of total strain energy release rate. The dimension of the smallest mesh used in calculation is 1% of the half crack length, *a*. Abaqus/Standard was used for FE analyses.

Results are shown in Table 2. It was found from the result that the stress intensity factors computed by both projection method and the displacement ratio method are accurate, especially in $K_I$, the dominant mode. On the other hand, there are slight disagreements in $K_{III}$ by the projection method. However, the magnitude of $K_{III}$ is approximately *3%* of the dominant mode. In cases when one mode is dominant over the other modes, stress intensity factors computed by the projection method in least dominant mode may not be accurate. Care must be taken when dominant mode is present. In such case, fracture driving force is represented by the dominant mode so the error in the least mode may not be important in actual applications.

It was found through comparison that the advantage of the projection method over the displacement ratio method, besides its simplicity, is that it does not require careful meshing strategies associated with calculations of total energy release rate. In addition, the stress intensity factors computed by the displacement ratio method depend on the node from which displacements were taken.

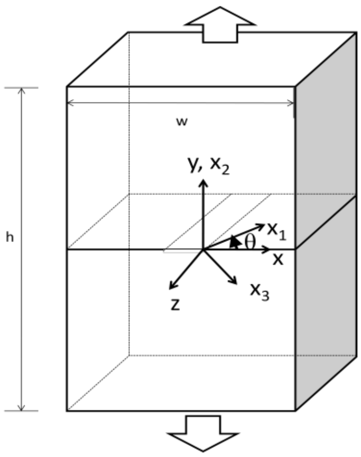


Fig. 2 Large body with a center crack along the interface under simple tension

Table 1 Stress intensity factors calculated for the large body with a center crack along the interface under simple tension

| $K_I/\sigma_{yy}^{\infty}\sqrt{\pi a}$ | | | | | |
|---|---|---|---|---|---|
| $[\theta_1/\theta_2]$ | Exact | Projection | Error(%) | Disp.Ratio | Error(%) |
| [0/90] | 1 | 1.009 | 0.9 | 0.9951 | 0.49 |
| [45/ − 45] | 1 | 1.0097 | 0.97 | 0.9804 | 1.96 |
| [0/45] | 1 | 0.9862 | 1.38 | 0.96643 | 3.36 |

| $K_{II}/\sigma_{yy}^{\infty}\sqrt{\pi a}$ | | | | | |
|---|---|---|---|---|---|
| $[\theta_1/\theta_2]$ | Exact | Projection | Error(%) | Disp.Ratio | Error(%) |
| [0/90] | -0.1343 | -0.1379 | 2.68 | -0.1358 | 1.12 |
| [45/ − 45] | 0 | 0 | −− | 0 | −− |
| [0/45] | -0.0892 | -0.09357 | 4.90 | -0.088 | 1.35 |

| $K_{III}/\sigma_{yy}^{\infty}\sqrt{\pi a}$ | | | | | |
|---|---|---|---|---|---|
| $[\theta_1/\theta_2]$ | Exact | Projection | Error(%) | Disp.Ratio | Error(%) |
| [0/90] | 0 | 0 | −− | 0 | −− |
| [45/ − 45] | -0.0765 | -0.0696 | 9 | -0.0765 | 3.01 |
| [0/45] | 0.0109 | 0.00672 | 38.3 | 0.0107 | 1.83 |

### 3.2 Uniform Edge Loadings

Consider [θ1//θ2] laminate with an edge delamination as shown in Fig. 3. The laminate is subjected to uniform edge loadings, $N_1$ and $N_2$. The laminate is assumed to be relatively long in *z*-direction. Under such condition, the stresses and strains are considered to be independent in *z*-direction so the problem can be simplified by assuming the generalized plane strain condition. Material properties of the ply used in this problem were $E_1=134.4GPa$, $E_2=E_3=10.2GPa$, $v_{12}= v_{13}=0.3$, $v_{23}=0.49$, $G_{12}=G_{13}=5.52GPa$, and $G_{23}=3.43GPa$. The applied edge loadings were $N_1= -50N/m$ and $N_2=80N/m$. The geometrical dimensions chosen for the analysis were $t_1=0.04$, $t_2=0.08$, and $a=b=0.96$. The 20-node brick element was used. The mesh was kept uniform near the crack tip, and the element size in the region was 0.1% of the crack length, *a*. The stress intensity factors calculated by the projection method were compared to those by the displacement ratio method proposed by Qian and Sun [1]. Fig. 4 illustrates how the projection method was used to compute stress intensity factors for this problem. Theoretically, it is expected that plots of the equation (3) are straight all the way to $x=0$ when plotted against the distance. However, Fig. 4 indicates that plots are not straight for first few elements. As mentioned previously, it is because stresses obtained from the finite element analysis are not accurate within the first few elements due to high stress gradients. Hence, projections must be taken by avoiding the region. Results are presented in Table 2. As it can be seen from the table, stress intensity factors computed by the projection method are in good agreements with those computed by the displacement ratio method.

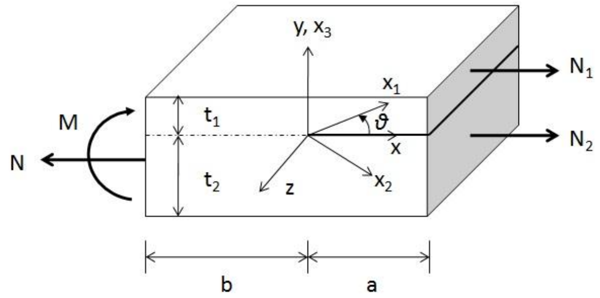


Fig. 3 Composite laminate with edge crack

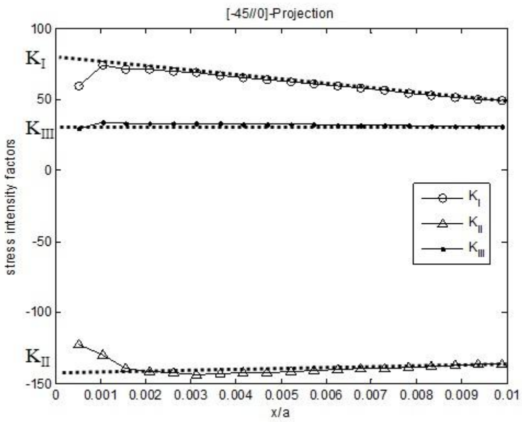


Fig. 4 Projection method used for the uniform edge loading problem

Table 2 Comparison of stress intensity factors from the projection method and displacement ratio method (DRM) for the uniform edge loading problem

| | $K_I$ | | $K_{II}$ | | $K_{III}$ | |
|---|---|---|---|---|---|---|
| | Projection | DRM | Projection | DRM | Projection | DRM |
| [0//-45] | 82 | 90.3 | -145 | -146.9 | 30.6 | 29 |
| [0//75] | 147.7 | 153.6 | -112.6 | -107.7 | -7.2 | -13.4 |
| [0//90] | 152.9 | 160.1 | -109 | -104 | 0 | 0 |

### 3.3 Uniform Stretching

It is well known that singular stress fields exist along the free edges of composite laminates. This stress singularity may cause free edge delamination. Consider a [-θ//θ/θ//-θ] laminate with free edge delamination under axial tensile loading in *z*-direction, as shown in Fig. 5.

The same material as the problem in the section 3.2 was used in numerical analyses. Because of symmetries, only a quarter portion of the entire body was modeled. The quarter cross-section is shown in Fig. 6. The crack length was selected to be $a=0.0254m$. The dimensions of the cross-section was chosen as follows; $t_1=0.04m$, $t_2=0.08m$, and $b=0.96m$. The 20-node brick element was used. The mesh was refined and kept uniform near the crack tip, and the mesh size was *0.1%* of $a$ in the region. Results are presented in Table 3. The stress intensity factors calculated by both methods agree very well in $K_{III}$, the dominant mode. It can be noted that there are slight mismatch in $K_{II}$. However, the mode mixities, $\varphi_{12}$ and $\varphi_{23}$, are in very good agreement. Therefore, the stress intensity factors calculated by the projection method can be still used to characterize fracture in this case.

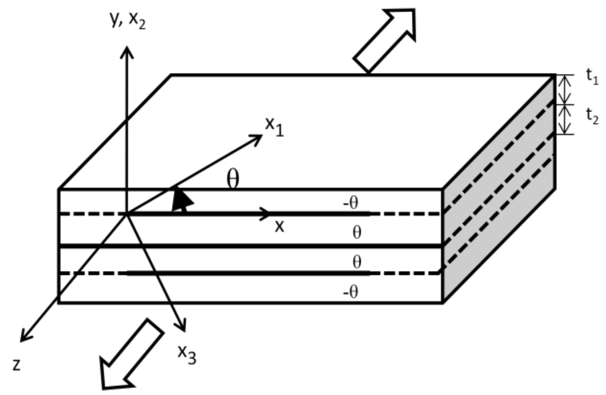


Fig. 5 A composite laminate with edge delamination along [−θ/θ] interface. Uniform stretching along *z*-axis is applied

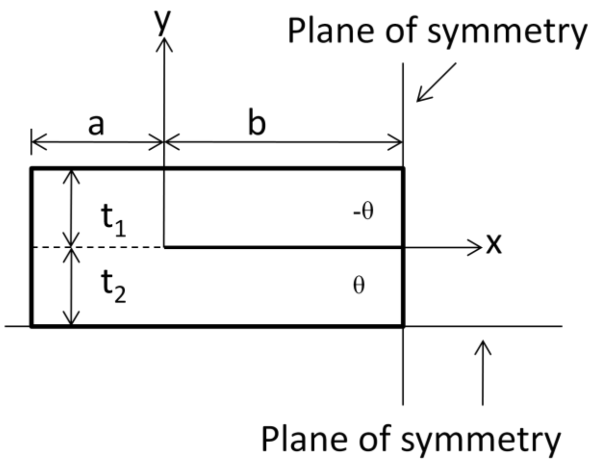


Fig. 6 A quarter of laminate cross-section

Table 3 Comparison of stress intensity factors from the projection method and displacement ratio method (DRM) for the uniform stretching problem

| | Projection | | | | |
|---|---|---|---|---|---|
| [-θ// θ/ θ// -θ] | $K_I$ | $K_{II}$ | $K_{III}$ | $\varphi_{12}$ | $\varphi_{23}$ |
| [-15//15/15//-15] | 0.75 | 0.0132 | 6.01 | 1.01 | 82.89 |
| [-45//45/45//-45] | 0.2303 | 0.0443 | -3.121 | 10.89 | -85.78 |
| [-75//75/75//-75] | 1.026 | -0.0237 | 43.34 | -1.32 | 88.64 |

| | DRM | | | | |
|---|---|---|---|---|---|
| [-θ// θ/ θ// -θ] | $K_I$ | $K_{II}$ | $K_{III}$ | $\varphi_{12}$ | $\varphi_{23}$ |
| [-15//15/15//-15] | 1.05 | 0.0183 | 6.03 | 1.00 | 80.12 |
| [-45//45/45//-45] | 0.2266 | 0.0636 | -3.04 | 15.68 | -85.74 |
| [-75//75/75//-75] | 1.171 | -0.0403 | 46.87 | -1.97 | 88.57 |

## 4 Conclusions

In this paper, the projection method was proposed for calculations of stress intensity factors for a delamination in composite laminates. The most significant feature of the method is its simplicity. It does not require complex mathematics, and involves fewer procedures compared to other methods. It was also shown that the method yields accurate stress intensity factors.

## References

[1] W. Qian and C.T. Sun “Calculation of stress intensity factors for interlaminar cracks in composite laminates”. *Composite Science and Technology*, Vol. 57, pp 637-650, 1997.

[2] H.C. Cao and A.G. Evans “An experimental study of fracture-resistance of bimaterial interface”. *Mechanics of Materials*, Vol.7, pp 295-304,1989.

[3] C.Hwu “Explicit solutions for collinear interface crack problems”. *International Journal of Solids and Structures*, Vol.3, pp 301-312, 1993

[4] A.H. England “A crack between dissimilar media”. *Journal of Applied Mechanics*, Vol 32, pp400-402, 1965

[5] M. Comninou “The interfacial crack”. *Journal of Applied Mechanics*, Vol.45, pp.287-290, 1978.

[6] J.R. Rice “Elastic fracture mechanics concepts for interfacial cracks”. *Journal of Applied Mechanics*, Vol.55, pp.98-103, 1988.

[7] C.T. Sun and Q. Qian “The use of finite extension strain energy release rates in fracture of interfacial cracks”. *International Journal of Solids and Structures*, Vol. 34, pp.2595-2609, 1997.